Micromagnetic modeling of the heat-assisted switching process in high anisotropy FePt granular thin films EP

Lewis J. Atkinson, Richard F. L. Evans (iD), and Roy W. Chantrell (iD)

COLLECTIONS

EP   This paper was selected as an Editor's Pick

View Online   Export Citation   CrossMark

Micromagnetic modeling of the heat-assisted switching process in high anisotropy FePt granular thin films ⓔⓟ

Lewis J. Atkinson, Richard F. L. Evans, ⓘⒹ and Roy W. Chantrell[a] ⓘⒹ

AFFILIATIONS

Department of Physics, University of York, Heslington, York YO10 5DD, United Kingdom

[a]**Author to whom correspondence should be addressed:** roy.chantrell@york.ac.uk

ABSTRACT

The dynamic process of assisted magnetic switchings has been simulated to investigate the associated physics. The model uses a Voronoi construction to determine the physical structure of the nanogranular thin film recording media, and the Landau–Lifshitz–Bloch equation is solved to evolve the magnetic system in time. The reduction of the magnetization is determined over a range of peak system temperatures and for a number of anisotropy values. The results show that the heat-assisted magnetic recording process is not simply magnetization reversal over a thermally reduced energy barrier. To achieve full magnetization reversal (for all anisotropies investigated), an applied field strength of at least 6 kOe is required and the peak system temperature must reach at least the Curie point (T_c). When heated to T_c, the magnetization associated with each grain is destroyed, which invokes the non-precessional linear reversal mode. Reversing the magnetization through this linear reversal mode is favorable, as the reversal time is two orders of magnitude smaller than that associated with precession. Under these conditions, as the temperature decreases to ambient, the magnetization recovers in the direction of the applied field, completing the reversal process. Also, the model produces results that are consistent with the concept of thermal writability; when heating the media to T_c, the smaller grains require a larger field strength to reverse the magnetization.

Published under license by AIP Publishing. https://doi.org/10.1063/1.5143120

I. INTRODUCTION

The increase in magnetic storage (areal) density over the past 60 years has been truly remarkable and is comparable with the much quoted increase in transistor device density—Moore's law. The increase in areal density has in the main resulted from adherence to geometric scaling[1,2] as the characteristic dimensions of the bits have been reduced over successive time intervals, although other factors have an impact on the increase in areal density, such as the change from longitudinal to perpendicular recording. Currently, information is recorded on a length scale of nanometers. At such length scales, the thermal stability of the magnetic components within the recording media is an increasingly significant problem due to the onset of superparamagnetic effects.[3] For a usable storage lifetime, the following inequality must be satisfied.

$$n_0 = \frac{K_u V}{k_B T} > 60, \quad (1)$$

where n_0 is the thermal stability factor. The historic solution to maintaining this inequality, when reducing the size of the magnetic components, has been to use materials with a larger bulk perpendicular magnetocrystalline anisotropy (K_u), which are thermally stable at a smaller volume (V).[1] However, the maximum output field of the inductive write head is determined by the material limit of the highest saturation magnetization found in magnetic solids, $\mu_0 M_s \sim 2.5$ T.[1,4] Therefore, K_u cannot be scaled up to the desired level to maintain n_0, since the write field required to reverse the magnetization will soon exceed the maximum output field of the inductive write head. Therefore, the maximum value of K_u is limited by the capability of write head technologies.[1]

A possible solution could use the fact that the anisotropy energy of a ferromagnetic material decreases with temperature, tending to zero as the temperature approaches the Curie point (T_c).[1,5] Therefore, n_0 can be varied from a condition of media stability at ambient temperature to approximately zero at temperatures approaching T_c. Thus, the temperature of the storage material can be raised locally and

momentarily, solving the problems of writability via the low-anisotropy state, with thermal stability being regained on cooling back to ambient temperature. This technique would allow for increasingly small grains to be used in the storage medium, leading to an increase in the areal density.[5] One technology that aims to use this approach is heat-assisted magnetic recording (HAMR).

The L1$_0$ ordered FePt, granular thin film is one of the most promising candidates for HAMR media due to its high bulk perpendicular magnetocrystalline anisotropy constant $K_u(0) = 9.0 \times 10^7$ ergs/cc[4] and a relatively low Curie temperature. HAMR is presently moving toward practical realization; recent work[6] having achieved a demonstrated areal density of 1.4 Tbit/sq in, for the first time, overtaking the densities achieved in conventional perpendicular recording. Despite this, the physical reliability of the HAMR process for realistic media is poorly understood, particularly considering the effects of grain size and its distribution and the importance of the anisotropy and intergranular exchange on the reversal process.

In this paper, we present a study of the magnetization dynamics of a FePt granular thin film during the HAMR process. An important factor in the model is the use of the Landau–Lifshitz–Bloch (LLB) equation to model the magnetization dynamics of the individual FePt grains within the thin film. The LLB equation has been used in place of the historically used the Landau-Lifshitz-Gilbert (LLG) equation, as it better describes the magnetization dynamics at elevated temperatures, close to T_c.[7] Importantly, the LLB equation allows magnetization reversal via the linear reversal mechanism,[8,9] which is important at temperatures close to T_c. The reversal process of the thin films magnetization and individual grains are investigated over a range of values for K_v and maximum temperatures.

We show that the HAMR process is not as simple as magnetization reversal within a reduced anisotropy regime. The reversal of the thin film magnetization is only achieved where the temperature is raised to T_c, and the applied field is sufficient to overcome the thermal excitation introduced via the heat assist.

II. THEORETICAL MODEL

To investigate the HAMR process, a model has been developed that replicates the physical structure of the granular recording medium, correctly describes the magnetization dynamics over a broad temperature range, and includes any granular interactions.

A. Magnetization dynamics: The Landau–Lifshitz–Bloch equation

The dynamics of the magnetization of each individual grains are modeled as single macrospins, using the Landau–Lifshitz–Bloch (LLB) equation. The LLB equation is capable of modeling the magnetization $\mathbf{m}_i$ of ferromagnetic nanoparticles on the sub-pico-second time scale and at temperatures up to and above T_c[10,11] and is here given in the stochastic form proposed by Evans et al.,[12] as

$$\dot{\mathbf{m}}_i = -|\gamma|[\mathbf{m}_i \times \mathbf{H}_{\text{eff}}^i] + \frac{|\gamma|\alpha_\parallel}{m_i^2}(\mathbf{m}_i \cdot \mathbf{H}_{\text{eff}}^i)\mathbf{m}_i$$
$$- \frac{|\gamma|\alpha_\perp}{m_i^2}\mathbf{m}_i \times [\mathbf{m}_i \times (\mathbf{H}_{\text{eff}}^i + \eta_\perp)]] + \eta_\parallel, \quad (2)$$

where $\alpha_\parallel = \lambda 2T/3T_c$ is the longitudinal damping parameter, $\alpha_\perp = \lambda(1 - T/3Tc)$ is the perpendicular damping parameter, γ is the gyromagnetic ratio, and λ is the intrinsic damping constant that couples the spin system to the heat bath at the atomistic level. Above T_c $\alpha_\parallel = \alpha_\perp = \lambda 2T/3T_c$. The effects of a non-zero temperature are introduced via a fluctuating magnetic field whose properties are determined by

$$\langle \eta_i^u \rangle = 0,$$
$$\langle \eta_i^\perp(0)\eta_j^\perp(t) \rangle = \frac{2k_B T(\alpha_\perp - \alpha_\parallel)}{|\gamma|M_s^0 V \alpha_\perp^2}\delta_{ij}\delta(t),$$
$$\langle \eta_i^\parallel(0)\eta_j^\parallel(t) \rangle = \frac{2|\gamma|k_B T \alpha_\parallel}{M_s^0 V}\delta_{ij}\delta(t), \quad (3)$$
$$\langle \eta_i^\parallel \eta_j^\perp \rangle = 0,$$

and $\mathbf{H}_{\text{eff}}$ is the sum of the applied, anisotropy, Zeeman and any interaction fields, which here includes the dipole approximation to the magnetostatic field and the intergranular exchange interaction.

The dynamics of the individual grains are calculated using the Heun scheme to numerically integrate the LLB equation. The parameters for the LLB equation [$M_s(T)$ and the longitudinal and transverse susceptibilities] are that of FePt and are determined from atomistic calculations using a multi-scale approach.[13] The Curie temperature is set to 660 K and damping parameter λ is set to 0.1 at $T = 0$ K, typical of granular recording media.[14–16] We note that recent experimental measurements have suggested a decrease in the measured ferromagnetic resonance linewidth, usually associated with a decrease in the intrinsic Gilbert damping.[17] However, the size distribution has been found to be the origin of this effect, and atomistic calculations confirm the divergence of the effective damping close to T_c[18] as assumed in our LLB model.

B. Thin film structure: The Voronoi construction

The model uses a Voronoi construction to produce the granular microstructure of the thin film. The Voronoi construction produces a physically realistic picture of the film, including a grain size dispersion and some microstructural disorders. The model generates three-dimensional grains 3–10 nm in diameter and height, each assumed magnetically to behave as a single domain. The easy axis for each of the grains is aligned with the z-axis. The Voronoi construction produces a film with the dispersion of grain size that is approximately lognormal. The standard deviation σ_v can be varied by changing the degree of randomness of the seed points for the Voronoi construction. Here, we studied a system approximately 600 nm × 600 nm ×5 nm in size and consisting of 7558 grains with periodic boundary conditions and a grain size distribution of $\sigma_v \sim 0.35$ for all simulations. The local field acting on the grain is calculated as follows:

$$\mathbf{H}_{eff}^i = \mathbf{H}_{applied} + \sum_{i \neq j}\frac{\mu_j}{r_{ij}^3}(3(\hat{r}_{ij} \cdot \hat{\mu})\hat{r}_{ij} - \hat{\mu}_j) + \mathbf{H}_e^i - \frac{(m_x^i e_x + m_y^i e_y)}{\chi_\perp}$$
$$+ \begin{cases} +\frac{1}{\tilde{\chi}_\parallel}\left(1 - \frac{m_i^2}{m_e^2}\right)\mathbf{m}_i & T \lesssim T_c \\ -\frac{1}{\tilde{\chi}_\parallel}\left(1 + \frac{3}{5}\frac{T_c}{T-T_c}m_i^2\right)\mathbf{m}_i & T \gtrsim T_c \end{cases}, \quad (4)$$

where $\mathbf{H}_{applied}$ is the (spatially uniform) external applied field which is set in the negative z direction throughout. The second term on the RHS of Eq. (4) is the dipole approximation to the magnetostatic term, which is calculated as a direct pairwise summation within a cutoff radius of 8 grain diameters, with long-range effects introduced via a mean field. The remaining terms in Eq. (4) are the contributions from the intergranular exchange, the anisotropy, and the intragranular exchange energy resulting from thermally induced longitudinal fluctuations of the magnetization.

The intergranular exchange interaction is formulated as in the work of Peng et al.[19] under the assumption that the exchange energy is proportional to the contact area between neighboring grains. The approach also allows for a dispersion in the exchange J_{ij} due to variations in grain boundary thickness and composition. In terms of reduced parameters (relative to the median values L_m, A_m, and J_m),

$$\mathbf{H}_e^i = H_{exch} \left(\frac{J_{ij}}{J_m}\right) \left(\frac{L_{ij}}{L_m}\right) \left(\frac{A_m}{A_i}\right) \hat{m}_j, \quad (5)$$

where L_{ij} is the contact length between grains i and j and A_i is the area of grain i in the plane of the thin film. In practice, H_{exch} is set by the requirement that the average exchange at saturation has a certain value H_{exch}^{sat}, that is,

$$H_{exch}^{sat} = H_{exch} \sum_i^N \sum_{j \in n.n} \left(\frac{J_{ij}}{J_m}\right) \left(\frac{L_{ij}}{L_m}\right) \left(\frac{A_m}{A_i}\right). \quad (6)$$

It is known that the intra-granular exchange decreases with increasing temperature, the effective field in a mean field approximation scaling with the magnetization. Here, we make a similar assumption. The exchange fields given during the later calculations refer to the 0 K value of the exchange field that is scaled appropriately in the model to represent the temperature reduction of the exchange.

III. RESULTS

Here, we are not aiming to simulate the detailed HAMR recording process; rather, the intention is to study the physics of HAMR as a field-cooled magnetization process, which casts light not only on the dynamics of HAMR but also on the thermodynamic aspects, limiting the recording densities in HAMR. Consequently, similar to the field, the temperature of the system is assumed spatially uniform. The anisotropy of the individual grains are modeled as a percentage of the bulk magnetocrystalline anisotropy constant, K_u, of $L1_0$ ordered FePt. This models a system in which each grain is partially $L1_0$ ordered, giving an anisotropy equal to a percentage of $L1_0$ ordered FePt. Each grain within the thin film has an equal K_u.

The initial study consists of simulations using the minimum anisotropy required to ensure the desired stability of the magnetization when applying Eq. (1) to a system comprised of grains with an average diameter of 6.0 nm, this equates to an anisotropy value of 1.8×10^7 ergs/cc, which is approximately 20% of the anisotropy of fully $L1_0$ ordered FePt. To observe the effect of increased temperature on the reversal process, quasi-static hysteresis curves, equivalent to Vibrating Sample Magnetometry (VSM) measurements, were generated using this system, the results are given in Fig. 1.

The quasi-static hysteresis curves were generated with a field sweep rate below which the observed hysteresis curves did not change—this was found to be approximately 100 Oe/ns after a equilibration period in the high field environment of 1.0 ns. As expected, the field required to reverse the magnetization is reduced as the temperature (T) is increased.

At ambient temperature (300 K), the system requires an applied field in the region of 25 kOe to reverse approximately 95% of the magnetization; clearly, the medium cannot be switched using conventional methods. These results are in agreement with the conventional picture of HAMR as magnetization reversal over a thermally reduced energy barrier, although this does not show the full complexity of the HAMR process; as the maximum temperature reached approaches T_c, the field required to reverse the magnetization is seen to increase and is of the same order as observed at ambient temperature. This is a reflection of the "thermal writeability" introduced by Evans et al.,[20,21] which quantifies the tendency of backswitching of magnetization at elevated temperatures.

Figure 1 presents measurements over a relatively long timescale; however, HAMR differs in nature from these hysteresis experiments as the temperature is raised only momentarily and the reversal process occurs during the subsequent cooling. This process is better investigated using an alternative measurement technique, first performed by Liu et al.,[22] where the magnetization is observed using a photomagnetic synchronized TR-MOKE technique, which resets the magnetic state to the initial conditions between each pump–probe experiment. Therefore, the photomagnetic synchronized TR-MOKE technique determines only the effect of the current laser pump and applied field, independent of the measurement history. It is essentially a single-shot technique with a characteristic timescale similar to that of the HAMR process. We have replicated this technique to better show the effect of the HAMR process. The temperature increase associated with the laser pulse is modeled as a step change from ambient temperature (300 K) to the
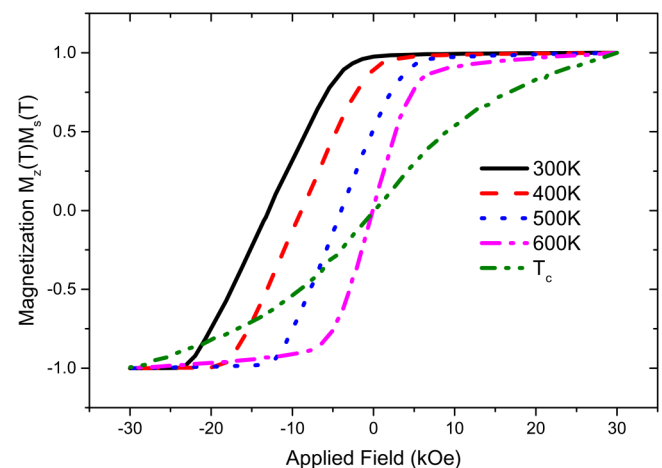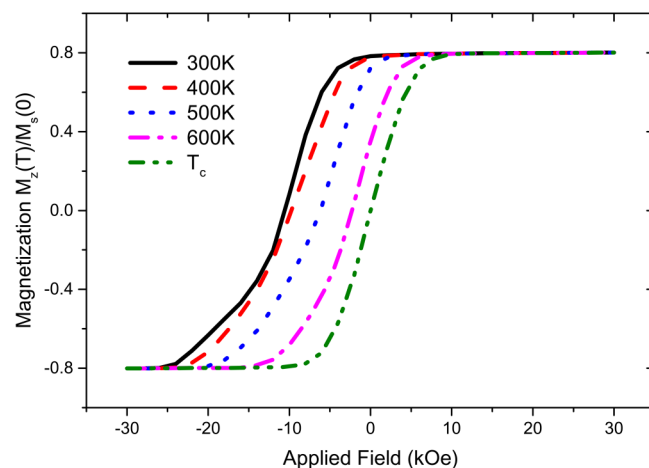

FIG. 1. Hysteresis curves generated with a thin film comprised of grains with an average diameter of 6.0 nm and with an anisotropy of the 20% $L1_0$ FePt case. These hysteresis curves show the effect of the increased temperature.
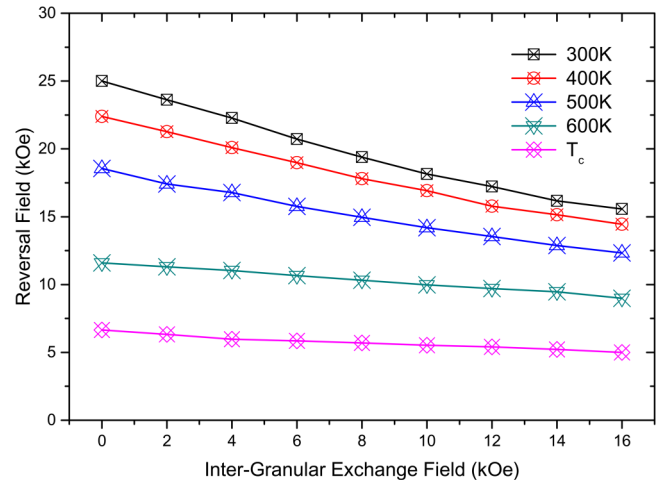
maximum temperature. The temperature then returns to ambient following a Gaussian form in a characteristic time and set to 0.5 ns throughout the investigation unless otherwise stated. With this cooling rate, the system temperature returns to ambient in ∼1.2 ns. All temperatures stated in the results section are given as the maximum temperature during the HAMR simulation. The decrease in the field required to reverse the magnetization can clearly be seen, in Fig. 2, reducing from approximately 25 kOe according to the standard hysteresis loop of Fig. 1 to 6 kOe using the measurement protocol of Liu *et al.*[22] Using this technique also indicates a reduction in the effect of the intergranular interactions with increasing T, as follows. At low temperatures the curves exhibit a change of gradient in the high negative field. This effect is usually interpreted as arising from the effects of the exchange and magnetostatic interactions, which drives the system into low energy states with low magnetization that are relatively stable and slow the approach to negative saturation. It can be seen in Fig. 2 that this effect is reduced with increasing temperature and is not present at the highest temperatures investigated.

The reduction of the effects of intergranular interactions at elevated temperatures is further demonstrated in Fig. 3. Here, the reversal field (defined as the field required to reverse 95% of the thin film magnetization) is given as a function of the intergranular exchange (IGE) field for a range of temperatures from ambient to T_c. The variation in the reversal field, due to increasing the IGE field, becomes less pronounced with increasing temperature, suggesting that the effect of the IGE field on the magnetization reversal process decreases with increasing temperature. This suggests that the intergranular interactions are not a significant contribution to the high-temperature magnetization processes involved in HAMR.

To further investigate the limits of the HAMR process the effects of K_u were further studied (Fig. 4). At ambient temperature, the reversal field is increased approximately linearly with increasing K_u, which neatly demonstrates the problem faced by hard disk
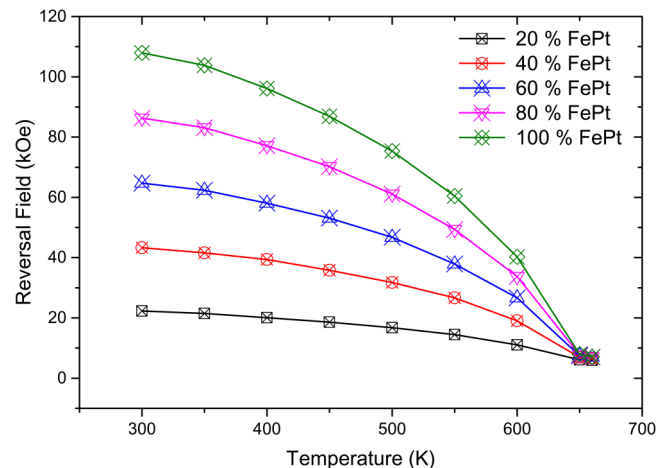

FIG. 3. The effect on the reversal field as a function of the exchange field and the maximum system temperature during the HAMR process. Note the reduced effect of the exchange field at higher maximum temperatures.

technologies. However, with a temperature rise to T_c, the reversal field is reduced to a similar level, for all values of K_u investigated, approximately 6 kOe.

This study of the hysteretic behavior confirms that increasing the temperature, as in the HAMR process, significantly reduces the field required to reverse the magnetization when compared with the ambient temperature. Also, the data have demonstrated that

FIG. 2. Hysteresis curves, using the alternate measurement technique developed by Liu *et al.* for the 20% L1$_0$ case, showing the effect of increasing the maximum temperature during the HAMR process.

FIG. 4. The effect on the reversal field as a function of the magnetocrystalline anisotropy (K_u) and as the maximum system temperature during the HAMR process. At ambient temperature, the field required to reverse the magnetization increases approximately linearly with increased K_u. Increasing the temperature to T_c during the HAMR process lowers the reversal to a similar level, 6 kOe, over the complete range of anisotropies investigated.

increasing the temperature reduces significantly the effects of the intergranular interactions and anisotropy field.

A. Dynamics of the HAMR process

HAMR is essentially a Field-Cooled Magnetization (FCM) process, albeit at extreme rates of temperature reduction and with a spatially and temporally varying magnetic field. This best characterizes the high-temperature switching of the magnetization and its eventual freezing into a stable state at a lower temperature.

Essentially, the HAMR process is not simply magnetization reversal over a thermally reduced energy barrier. Evans and Fan[23] have shown that, although thermally activated switching below the Curie temperature can result in switching, the timescale over which the temperature must remain constant is prohibitively long. It was suggested in Ref. 23 that reliable switching requires heating above T_c so as to activate the linear reversal mode (to be discussed in detail later) during cooling and an applied field strength sufficient to overcome the effects of thermal writability. Here, we investigate these thermodynamic aspects of the HAMR process with an emphasis on the effects of the dispersion of grain volume.

In order to investigate the underlying switching mechanisms involved in HAMR, we use a simplified picture in which the applied field is held constant as the temperature is changed using the same approach as described above when replicating the measurement method of Liu et al.[22] The effects of different levels of increased temperature and cooling rate are both determined. Figure 5 shows the M_z time sequences for the 20% and 100% L1$_0$ ordered FePt cases, where the applied field strength was 6 kOe throughout. We note that the magnetization is normalized to the saturation value at zero K. For the 20% FePt case at temperatures well below T_c, one can distinguish three distinct time regimes. Initially, there is a very rapid reduction of the magnetization,

driven by the rapid temperature increase. This involves longitudinal magnetization changes; i.e., the reduction in the magnitude of the magnetization of the grains. The longitudinal relaxation time is of the order of a few hundred fs, as shown by Chubykalo-Fesenko et al.,[7] and as a result the magnetization very rapidly follows the temperature increase. After this process, the magnetization proceeds by precessional switching over the thermally reduced energy barriers. Finally, as the temperature lowers there is a slower change in the magnetization caused by thermally activated reversal events which, depending on the grain size, can be significant out to 10–20 ns. The heat-assist effect is clear from the data presented. At ambient temperature, the field is insufficient to reverse a significant number of grains. As the temperature increases, increasing numbers of grains can be switched due to the reduction in the value of K_u.

This supports the conventional picture of HAMR as a process driven by thermal activation over thermally reduced energy barriers and applies to all peak temperatures considered up to 600 K. However, it is important to note that during these processes, the magnetization is not completely reversed. Complete reversal is observed only for temperatures $T \gtrsim 650$ K. This effect is even more pronounced in calculations for 100% ordered FePt, as shown in Fig. 5, where magnetization reversal is not seen even for temperatures as high as 600 K.
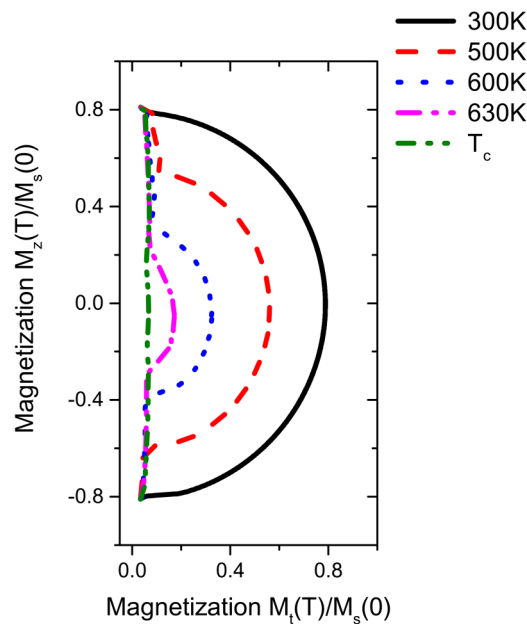
B. Linear reversal

It is also interesting to note that there is a significant change in behavior between peak temperatures of 640 K and 660 K. This can be interpreted as arising from the onset of the linear reversal mode;[8,9] which is characterized by ultrafast reversal via longitudinal magnetization changes. The transition to linear reversal is demonstrated in Fig. 6, which shows the longitudinal vs transverse magnetization throughout the reversal process for the low-anisotropy,
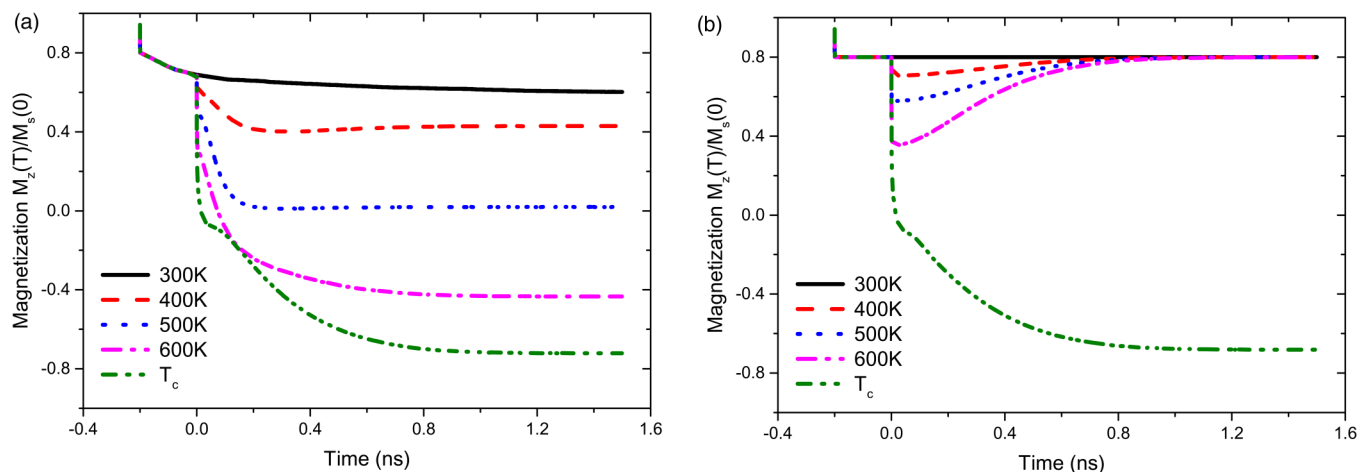
FIG. 5. (a) An M$_z$ time sequence for the thin film magnetization for the 20% L1$_0$ case, with a 6 kOe applied field throughout the simulation. The time sequence shows the effect of applying a temperature increase during the magnetization reversal process, and it also shows that the temperature must be increased to T_c to fully reverse the magnetization. (b) The M$_z$ time sequence for the thin film magnetization for the 100% L1$_0$ case again with a 6 kOe applied field. Note the higher anisotropy simulation requires a higher temperature increase to achieve the same level of magnetization reversal.

20% $L1_0$ ordered FePt, case. The results are consistent with the atomistic simulations given by Barker et al.[9] At low temperatures, the reversal is by coherent rotation, characterized by a constant magnitude of the magnetization throughout this process, with the magnetization magnitude decreasing with increased temperature. In this regime, the reversal is precessional with characteristic switching times in the order of 10–100 ps. However, above a temperature of 600 K reversal proceeds via a different, non-precessional, switching mechanism termed elliptical and linear reversal. While reversal proceeds by precession of individual spins at the atomistic level, the macroscopic spin associated with individual grains reverses via a reduction of the magnetization and, in the case of linear reversal, collapse of the magnetization through zero.

Within the temperature range of 600 K–640 K, the magnetization is seen to reverse through the elliptical reversal mode, where the magnetization decreases to a minimum magnitude in the anisotropy hard direction and then increases as the system temperature returns to ambient. This process gives the characteristic elliptical reversal pattern seen in Fig. 6 and importantly results in a reduced energy barrier relative to coherent reversal. Above a temperature of 640 K, reversal occurs via the linear reversal path, where the magnetization of the individual grains is effectively destroyed on heating and then rebuilds in the direction of the applied field as the system temperature returns to ambient. This mechanism is

extremely fast acting with characteristic times of the order of the longitudinal relaxation time of FePt (100 fs). The dynamical reversal process is illustrated in Fig. 7, which shows the M_z time sequence for an individual grain for a peak temperature of T_c and over a range of cooling rates. The magnetization vanishes and reverses rapidly as shown, after which the evolution of the magnetization essentially follows the time evolution of the temperature profile during the cooling process.

We now turn to the behavior of the ensemble of grains, particularly, investigating the effect of the cooling rate. The results are given in Fig. 8, which shows the time evolution of the magnetization after heating to T_c. For the lowest cooling rate cases, 0.2 ns and below, the magnetization of a portion of the grains remains in the initial orientation after the HAMR process. Complete reversal is only achieved for slow cooling rates. We interpret the data as arising from a "switching window" defined by the time between the appearance of the magnetization on cooling through T_c and the blocking temperature at which the magnetization freezes.

For illustration, we first present a simple model of HAMR as a Field-Cooled Magnetization (FCM), which is the magnetization achieved after a sample is cooled from a high-temperature state of zero magnetization, through its blocking temperature in an applied field. This is essentially the HAMR recording process, except that the sample may be cooled from above T_c. If we assume that the sample attains thermal equilibrium immediately on cooling through T_c, we can apply the semi-analytical approach of Chantrell and Wohlfarth,[24] with the provision that at each temperature, the saturation magnetization and anisotropy must be reevaluated. In Ref. 24, it was shown that the FCM is dependent on the rate of reduction of the temperature ($\dot{T}$). Essentially, the magnetization is assumed to be in thermal equilibrium above a rate dependent blocking temperature T_B, with the equilibrium magnetization being frozen in as the temperature is cooled through T_B. In Ref. 24, it was
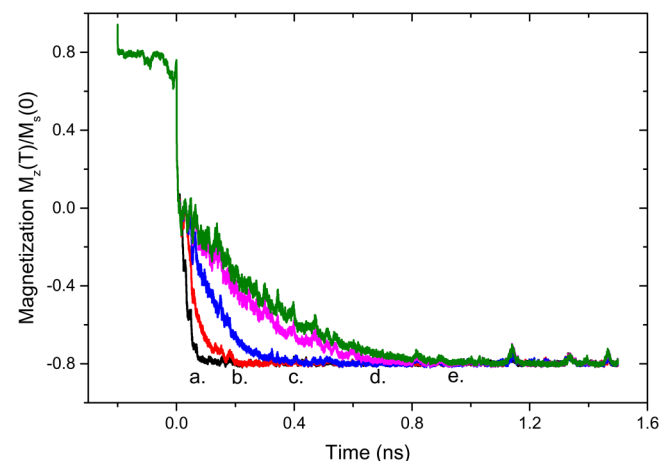

FIG. 6. The reversal mechanism of an individual grain magnetization (the data are presented as the transverse magnetization component vs the z magnetization component) for the 20% $L1_0$ ordered case over a range of maximum system temperatures. The change in reversal modes is clearly displayed from a strictly precessional type with a maximum temperature below 550 K through the elliptical mode as the temperature approaches T_c and onto the linear reversal mode at temperatures above 650 K.

FIG. 7. The linear reversal case (heating to T_c) for a single grain over a range of cooling rates. The reversal of the individual grain magnetization is seen to happen at a greater rate with the quicker cooling time. The cooling times are as follows: (a) 0.05 ns, (b) 0.1 ns, (c) 0.2 ns, (d) 0.4 ns, and (e) 0.5 ns.
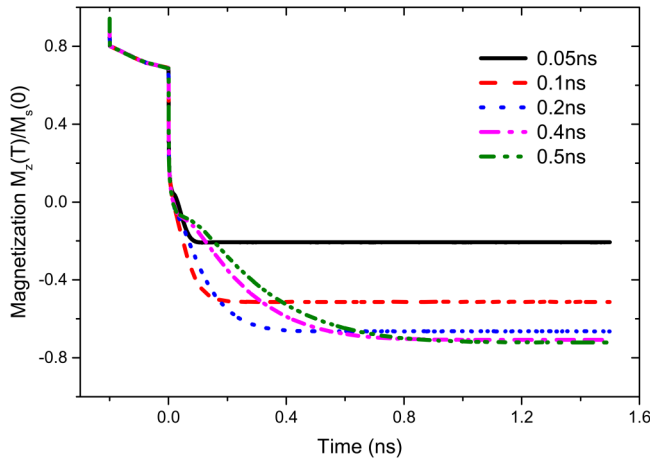
FIG. 8. The time variation of the magnetization after heating to T_c for the thin film magnetization over a range of cooling rates. For a cooling rate below 0.2 ns, the level of magnetization reversal is significantly reduced.

shown that the rate dependent blocking temperature is determined via the parameter Z_c, given as a solution of the equation

$$Z_c = \ln{(\dot{T}25f_0 T_K(1-h)^2/Z_c^2)}, \qquad (7)$$

where $Z_c = \frac{K_u V}{k_B T_B}(1-h)^2$, $T_K = K_u V/25 k_B$ is the blocking temperature for quasi-static measurements, and h is the reduced field H/H_K. From Eq. (7), T_B is given as

$$T_B = \frac{K_u V}{k_B Z_c}(1-h)^2. \qquad (8)$$

In Ref. 24, the blocking temperature was calculated in an analytical approximation, but here we will use a numerical solution of Eq. (7). Consider a monodisperse ensemble of particles (diameter D) with aligned easy axes, an anisotropy constant K_u, and saturation magnetization of M_s. According to Ref. 24, within the blocking model, the system is assumed to be in thermal equilibrium for $T > T_B$ and makes a transition to non-equilibrium behavior at T_B. Given that the thermal equilibrium magnetization for an aligned system is $M = \tanh{\beta}$ with $\beta = M_s V H/k_B T$, we have that

$$M = \tanh{\beta} \quad (T > T_B) \qquad (9)$$

and

$$M = \tanh{\beta_c} \quad (T \le T_B), \qquad (10)$$

where $\beta_c = M_s V H/k_B T_B$. Equation (10) reflects the fact that the magnetization below T_B remains at the value frozen in at T_B. To calculate $K_U(T)$, the Callen–Callen theory is used. Given the temperature dependences of K_u and M_s, it is straightforward to calculate $M(T)$ using Eqs. (7)–(10). The FCM has been calculated as a function of the grain size, applied field, and cooling rate.

Figure 9 shows the variation of the FCM with temperature for a variety of parameters and a cooling rate of 500 Kns^{-1}. The data presented are for a number of particle sizes and applied field strengths. For the 500 nm^2 sized particle in a field of 10 kOe, the magnetization varies smoothly with temperature. Whereas the smaller particles of 180 nm^2, the magnetization shows a change of slope at around 450 K, indicating the onset of blocking. This is more pronounced in the final set of data in a smaller field of 5 kOe. While the semi-analytical approach reproduces the form of the recovery of the magnetization on cooling, it does not reproduce the reduction of the switched magnetization at high sweep rates evident in Fig. 8.

This is due to the very rapid cooling under these conditions, which causes the system to go from the high-temperature–low-anisotropy regime, where magnetization reversal can occur, to the low temperature–high anisotropy regime where reversal is forbidden, in a period of time which is too fast to allow the system to reach thermal equilibrium at each temperature. This result is a dynamic generalization of the concept of "thermal writability," suggesting that cooling rates should be sufficiently slow as to allow the magnetization to equilibrate. We can quantify this in terms of the freezing time related to the temperature sweep rate R_T as follows; $\tau_f = (T_c - T_B)/R_T$, essentially τ_f is the time between the Curie temperature and the blocking temperature. For efficient switching in HAMR, $\tau_r < \tau_f$, where τ_r is the relaxation time of the magnetization during the cooling process. This stresses the importance of the linear reversal mechanism,[9,25] which gives access to relaxation times of the order of picoseconds.[23]

## C. Grain volume

Further insight into the HAMR process is gained by investigating the reversal process as a function of the grain volume and
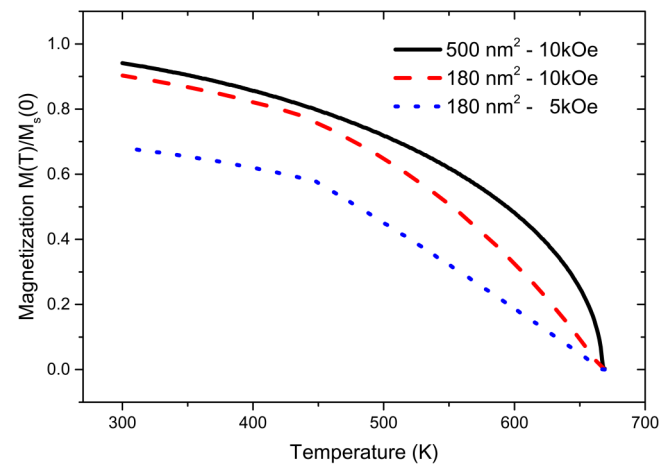
FIG. 9. Field-cooled magnetization curves as a function of particle sizes 180 nm^2 (900 nm^3) and 500 nm^2 (2500 nm^3) and magnetic field. The cooling rate is 500 K ns^{-1}. The system becomes increasingly blocked as the size of both particle field and applied field is reduced.
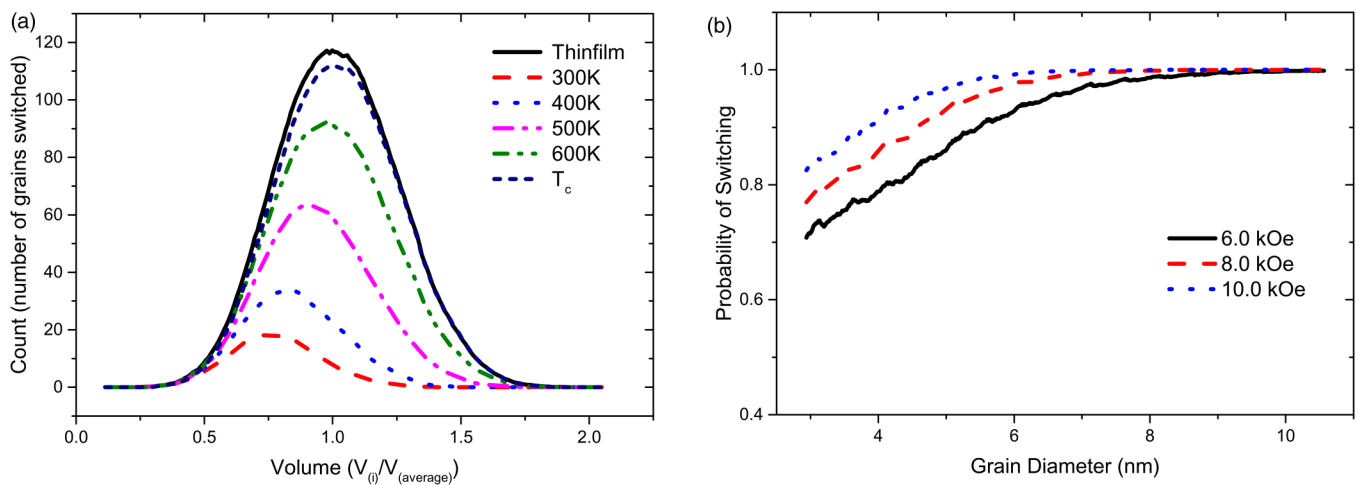
FIG. 10. (a) The spread of the relative volume of the FePt grains within the thin film, showing the spread of the volume for the grains which have reversed the magnetization after the HAMR process over a range of maximum system temperatures. "Thin film" denotes the intrinsic size dispersion of the system. (b) The reversal percentage for the 100% $L1_0$ ordered thin film, where the temperature was raised to T_c during the HAMR process. Below a critical grain size the probability of the magnetization reversing is significantly reduced for a given applied field strength, where the critical grain size is reduced with increased field strength.

temperature as shown in Fig. 10(a). Here, the number of grains reversed for a given volume at each a maximum temperature is given. Figure 10 demonstrates that the smaller grains are reversed at lower temperatures, with an increasing fraction of the large grains reversed at elevated temperatures. This result is again consistent with the conventional view of HAMR, as increasing the temperature lowers the anisotropy further allowing for ever larger grains to reverse. However, it is interesting to note that between peak temperatures of 600 K and 660 K, there is a significant increase in the number of grains switch with no corresponding large increase in the mean diameter switched. This is likely due to access to the elliptical and linear reversal modes in this region, which will assist the system in reaching thermal equilibrium values for the magnetization.

Our results also demonstrate the effects of the concept of the "thermal writability,"[20,21] which introduces the requirement that the write field H_{wr} should be sufficiently large not only to switch the magnetization but also to ensure that at the freezing temperature (T_f) of the grains $(M_s(T)V)$ is large enough to ensure that there is no thermally induced backswitching of the magnetization. This is demonstrated in Fig. 10(b) where the probability of reversal is significantly reduced below a critical grain size. The critical grain size decreases with increasing field strength, indicating an increase of the blocking temperature for a fixed grain size. Practically, this is notable for two reasons. First, it suggests that smaller grains will create increased dc noise. Second, we note that the switching field of 10 kOe is not sufficient to fully switch grains of less than around 5 nm in diameter, which confirms the prediction of Evans et al.[20] that thermal writability is a more stringent criterion than that of thermal stability given that FePt grains as small as around 3.3 nm in diameter[26] are thermally stable according to the usual criterion $K_u V/(k_B T) = 60$.

D. HAMR implications

In terms of applications in recording, the final state of the system after the HAMR process is of central importance. Here, we characterize the final state in terms of a reversal probability, taken as the reduced magnetization (relative to saturation), after the HAMR process. Figure 11 shows the reversal probability over a range of anisotropy values and maximum system temperatures. This clearly shows the increase in the temperature required to initiate the reversal process in the higher anisotropy simulations. Above an anisotropy of 60%, $L1_0$ ordered grains and below a temperature of 600 K, the system shows very low or zero magnetization reversal. The data also show that, when the maximum system temperature reaches T_c, reversal is achieved for all anisotropy values. For the relatively low-anisotropy values, it can be seen that there is a relatively weak dependence of the reversal probability, although the probability does increase up to T_c. There is a much more dramatic effect of temperature for values of anisotropy approaching that of bulk FePt. Here, peak temperatures as high as 640 K are not sufficient to cause switching of the magnetization; a switching path is only available via linear reversal, which suggests that this mechanism will increasingly become the dominant process as the anisotropy value increases in line with the requirement of thermal stability at ultra-high densities.

These two constraints, the higher anisotropy regimes needing increasingly higher temperatures (approaching T_c) to initiate reversal, mean that the temperature range where reversal is seen is reduced as the anisotropy is raised. This is a significant result for HAMR, as a narrower range of temperature where magnetization reversal is seen implies the reversal process must take place over a smaller timescale dictated by the timescale where the system temperature is at T_c. This could lead to the possibility of incomplete switching, as reversal must occur at this high temperature. In this
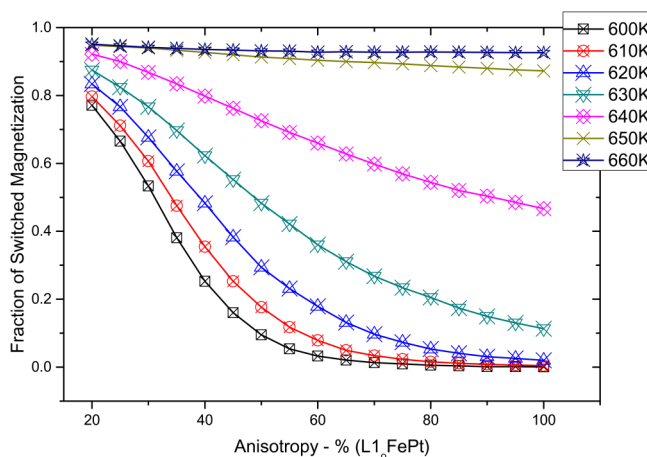
FIG. 11. The reversal probability of the thin film magnetization with a 6 kOe applied field over a range of maximum system temperatures (600 K−T_c) and anisotropies (20%–100% bulk L1$_0$ ordered FePt grains).

respect, the intrinsically fast (ps timescale) of switching via linear reversal is an important factor.

IV. CONCLUSION

We have investigated the physics of the HAMR process, a viable extension to hard disk magnetic data storage technologies. As expected, the field required to reverse the magnetization of a given granular thin film sample is reduced with increased temperature. However, we have shown that the HAMR process is not simply magnetization reversal over a thermally reduced energy barrier in the high-temperature/low-anisotropy regime but far more complex. To reverse, the magnetization via the HAMR process requires that the temperature has to be raised close to T_c for all anisotropies investigated and that the write field (H_{wr}) must be sufficient not only to reverse the magnetization but also to overcome backswitching due to the excess thermal energy associated with the HAMR process.

At temperatures sufficiently below T_c, in the case of FePt $T \leq 600$ K, the individual grains are seen to reverse through three stages: first, a reduction in the magnitude of the magnetization associated with the rapid temperature rise. Then, the reversal occurs over the reduced anisotropy, as in the conventional view of HAMR, where the anisotropy has been sufficiently reduced to allow precessional reversal over the reduced energy barrier. Finally, as the temperature lowers, there is a slower change in the magnetization caused by thermally activated reversal events which, depending on the grain size, can be significant out to 10–20 ns. These effects are anisotropy dependent, and therefore, the temperatures where these effects are seen are much larger for the higher anisotropy regimes, and in this fashion, the magnetization of the thin film is not fully reversed. At higher temperatures, the linear reversal comes into play, giving a faster route to achieve the thermal equilibrium magnetization, which thermodynamically is the maximum possibility.[20]

We have demonstrated that to set the magnetization to the preferred direction, via the HAMR process, the temperature must be raised to T_c and the applied field must be sufficient to overcome the superparamagnetic freezing associated with the rapid temperature decrease. This implies that magnetic recording, via HAMR, is only possible through the newly proposed linear reversal mode, where the magnetization is entirely destroyed by the temperature increase to T_c and then is rebuilt in the direction of the applied field as the temperature returns to ambient. We find that the thermal writability factor[20] is an important limitation in HAMR. Our simulations show that at diameters below around 5 nm backswitching becomes increasingly important, suggesting that thermal writability is a more stringent limitation than thermal stability since fully ordered grains as small as 3.3 nm are expected to be thermally stable. However, we note that our calculations assume a value of 10 kOe for the switching field. While this is realistic for current technology, it suggests that the introduction of higher effective fields such as are available through, for example, thermally induced magnetization switching[27] will be necessary for magnetic recording to achieve its full potential. In relation to switching of FePt, it has been shown that all-optical switching has been observed.[28–31] However, the mechanism appears to be via an accumulated reversal over many pulses that are consistent with the relatively low magnetization values achieved and suggests that this mechanism is not feasible for practical recording processes.

DATA AVAILABILITY

The data that support the findings of this study are available within the article.

REFERENCES

[1]T. W. McDaniel, J. Phys. Condens. Matter **17**, R315 (2005).
[2]R. Wood, IEEE Trans. Mag. **36**, 36 (2000).
[3]J. Bean and C. P. Livingston, J. Appl. Phys. **S30**, 120S (1959).
[4]S. D. Granz and M. H. Kryder, J. Magn. Magn. Matter **324**, 287 (2012).
[5]O. Heinonen and K. Z. Gao, J. Magn. Magn. Matter **320**, 2885 (2008).
[6]G. Ju, Y. Peng, E. K. C. Chang, Y. Ding, A. Q. Wu, X. Zhu, Y. Kubota, T. J. Klemmer, H. Amini, L. Gao, Z. Fan, T. Rausch, P. Subedi, M. Ma, S. Kalarickal, C. J. Rea, D. V. Dimitrov, P. W. Huang, K. Wang, X. Chen, C. Peng, W. Chen, J. W. Dykes, M. A. Seigler, E. C. Gage, R. Chantrell, and J. U. Thiele, IEEE Trans. Mag. **51**, 1–9 (2015).
[7]O. Chubykalo-Fesenko, U. Nowak, R. W. Chantrell, and D. Garanin, Phys. Rev. B **74**, 094436 (2006).
[8]N. Kazantseva, D. Hinzke, R. W. Chantrell, and U. Nowak, Europhys. Lett. **86**, 27006 (2009).
[9]J. Barker, R. F. L. Evans, R. W. Chantrell, D. Hinzke, and U. Nowak, Appl. Phys. Lett. **97**, 192504 (2010).

[10]D. A. Garanin, Phys. Rev. B **55**, 3050 (1997).

[11]D. A. Garanin and O. Chubykalo-Fesenko, Phys. Rev. B **70**, 212409 (2004).

[12]R. F. L. Evans, D. Hinzke, U. Atxitia, U. Nowak, R. W. Chantrell, and O. Chubykalo-Fesenko, Phys. Rev. B **85**, 014433 (2012).

[13]N. Kazantseva, D. Hinzke, U. Nowak, R. W. Chantrell, U. Atxitia, and O. Chubykalo-Fesenko, Phys. Rev. B **77**, 184428 (2008).

[14]N. Mo, J. Hohlfeld, M. ul Islam, C. Scott Brown, E. Girt, P. Krivosik, W. Tong, A. Rebei, and C. E. Patton, "Origins of the damping in perpendicular media: Three component ferromagnetic resonance linewidth in Co–Cr–Pt alloy films," Appl. Phys. Lett. **92**, 022506 (2008).

[15]X. Ma, L. Ma, P. He, H. B. Zhao, S. M. Zhou, and G. L upke, "Role of antisite disorder on intrinsic Gilbert damping in $L1_0$ FePt films," Phys. Rev. B **91**, 014438 (2015).

[16]K.-D. Lee, H.-S. Song, J.-W. Kim, H. S. Ko, J.-W. Sohn, B.-G. Park, and S.-C. Shin, "Gilbert damping and critical real-space trajectory of $L1_0$-ordered FePt films investigated by magnetic-field-induction and all-optical methods," Appl. Phys. Express **7**, 113004 (2014).

[17]D. Richardson, S. Katz, J. Wang, Y. Takahashi, K. Srinivasan, A. Kalitsov, K. Hono, A. Ajan, and M. Wu, "Near-Tc ferro- magnetic resonance and damping in FePt-based heat-assisted magnetic recording media," Phys. Rev. Appl. **10**, 054046 (2018).

[18]M. Strungaru, S. Ruta, R. F. L. Evans, and R. W. Chantrell, "Model of magnetic damping and anisotropy at elevated temperatures: Application to granular FePt films," Phys. Rev. Appl. **14**, 014077 (2020).

[19]Y. Peng, X. W. Wu, J. Pressesky, G. P. Ju, W. Scholz, and R. W. Chantrell, J. Appl. Phys. **109**, 123907 (2011).

[20]R. F. L. Evans, R. W. Chantrell, U. Nowak, A. Lyberatos, and H. Richter, Appl. Phys. Lett. **100**, 102402 (2012).

[21]H. J. Richter, A. Lyberatos, U. Nowak, R. F. L. Evans, and R. W. Chantrell, J. Appl. Phys. **111**, 033909 (2012).

[22]X. D. Liu, Z. Xu, R. X. Gao, Z. F. Chen, T. S. Lai, J. Du, and S. M. Zhou, J. Appl. Phys. **106**, 053907 (2009).

[23]R. F. L. Evans and W. J. Fan, Appl. Phys. Lett. **105**, 192405 (2014).

[24]R. W. Chantrell and E. P. Wohlfarth, Phys. Stat. Sol. **91**, 619 (1985).

[25]N. Kazantseva, D. Hinzke, R. W. Chantrell, and U. Nowak, Europhys. Lett. **86**, 27006 (2009).

[26]D. Weller and A. Moser, IEEE Trans. Magn. **35**, 4423 (1999).

[27]T. Ostler et al., Nat. Commun. **3**, 391 (2012).

[28]J. Y. Shi, X. F. Hu, M. Tang, J. Xu, L. Q. Shen, S. M. Zhou, X. J. Yang, Y. Z. Wu, L. Y. Chen, and H. B. Zhao, AIP Adv. **9**, 035039 (2019).

[29]R. John, M. Berritta, D. Hinzke, C. Müller, T. Santos, H. Ulrichs, P. Nieves, J. Walowski, R. Mondal, O. Chubykalo-Fesenko, J. McCord, P. M. Oppeneer, U. Nowak, and M. Münzenberg, Sci. Rep. **7**, 4250 (2017).

[30]Y. K. Takahashi, R. Medapalli, S. Kasai, J. Wang, K. Ishioka, S. H. Wee, O. Hellwig, K. Hono, and E. E. Fullerton, Phys. Rev. Appl. **6**, 3200904 (2016).

[31]M. Ellis, E. Fullerton, and R. Chantrell, Sci. Rep. **6**, 30522 (2016).